Proc. Nat. Acad. Sci. USA
Vol. 71, No. 11, pp. 4617–4621, November 1974

Restriction Endonuclease Cleavage Maps of Animal Mitochondrial DNAs

(electron microscopy/replication/human, monkey, and mouse mitochondrial DNAs)

WESLEY M. BROWN† AND JEROME VINOGRAD‡

†‡ Division of Biology and ‡ Division of Chemistry and Chemical Engineering, California Institute of Technology, Pasadena, Calif. 91125

Contributed by Jerome Vinograd, September 3, 1974

ABSTRACT **The restriction endonuclease, *Hin*dIII, gives rise to three fragments in each of the three mitochondrial DNAs isolated from the established mammalian cell lines LA9 (mouse), HeLa (human), and BSC-1 (African green monkey). The restriction endonuclease, *Eco*RI, gives rise to three fragments in mitochondrial DNA from HeLa and to two in DNAs from LA9 and BSC-1. The sizes and the orders of the fragments in the respective genomes have been determined with data obtained from the electron microscope. The origin and the direction of replication have been designated in each of the cleavage maps. Polyacrylamide gel electrophoretic analyses demonstrated that additional fragments not detectable in the electron microscope and larger than 50 nucleotide pairs were not present.**

The restriction endonucleases *Eco*RI from *Escherichia coli* (1) and *Hin*dIII from *Haemophilus influenzae* (1) recognize a different hexanucleotide sequence in DNA (1). Each produces a small number of specific fragments with mitochondrial DNAs (mtDNAs) isolated from established cell lines of human, African green monkey, and mouse origin. Because these DNAs contain D-loops at the origin of replication (2, 3), it is possible to develop cleavage maps of the fragments with the sites of the origin of replication as reference points. Since replication proceeds unidirectionally (4, 5), fragments obtained from larger replicating forms disclose the direction of replication on the map and refine the site of origin of replication to one fork of the D-loop. The development of six cleavage maps is described in this communication. It is anticipated that these maps will serve as primary maps for subsequent mapping studies.

MATERIALS AND METHODS

Cell Lines. The established lines were HeLa (human), BSC-1 (African green monkey), and LA9 (mouse). Woolly monkey primaries, derived from kidney tissue, were a gift from Dr. T. Kawakami, University of California, Davis. Cells were grown in suspension (HeLa and LA9) or on petri dishes (BSC-1 and woolly monkey), with Dulbecco's modification of Eagle's medium and, except for HeLa cells, 10% calf serum. For HeLa cells, 5% serum was used. Cells were harvested late in exponential growth.

Preparation and Purification of mtDNA. mtDNA was prepared from partially purified mitochondria as described in sections 2 (a) (i) and 2 (a) (iii) of ref 6. After velocity sedimentation, the DNA was recentrifuged to buoyant equilibrium in CsCl–propidium diiodide and fractionated by drop collection. The lower band fractions and those containing the region between the lower and upper bands were pooled separately. They were dialyzed against 100 volumes of 1.5 M NaCl–0.15 M sodium citrate containing 5% (w/v) Dowex 50 w-8 resin to remove dye, and then against a suitable buffer. mtDNA prepared in this manner and spread by the aqueous technique contained 90% supercoiled molecules; the remainder were open circular molecules of mtDNA size. Linear molecules were rarely seen in these preparations.

Enzymes. *Eco*RI endonuclease was a gift from Dr. Herbert Boyer, University of California Medical Center, San Francisco. *Hin*dIII endonuclease and *E. coli* polymerase I were gifts of Dr. Paul Johnson, California Institute of Technology. The enzymes did not linearize ϕX174 replicative form (RF) DNA, which does not contain the sites for cleavage, even when incubated with a 10-fold excess of enzyme and for times 5-fold longer than necessary to completely cleave mtDNAs.

Glyoxal Fixation and Enzymatic Restriction of mtDNA. A solution containing mtDNA in 0.2 M potassium phosphate (pH 7.0) was made 0.5 M in glyoxal (40% aqueous solution; Matheson, Coleman and Bell) and incubated at 37° for 60 min. The reaction mixture was then dialyzed against the appropriate restriction buffer at 25°, with two buffer changes at 1-hr intervals. The *Eco*RI restriction buffer used was 0.1 M Tris·HCl, 5 mM $MgCl_2$, 50 mM NaCl (pH 7.6). The buffer for *Hin*dIII was 50 mM NaCl, 10 mM Tris·HCl, 5 mM $MgCl_2$, 5 mM 2-mercaptoethanol (pH 7.6). Restriction of unfixed DNA was carried out in the same buffer.

Electron Micrographical Analysis of DNA Fragments. The DNA was spread with either aqueous or formamide spreading conditions (7). Grids were stained with alcoholic uranyl acetate and shadowed with Pt-Pd, as described (7). They were examined and photographed in a Philips 300 electron microscope at a (film) magnification of 3000×. Negatives were projected onto a Hewlett-Packard 9864 A Digitizer connected to a 9820 A calculator system and measured.

Either full-length mtDNA or ϕX174 RF DNA molecules were added to the samples after enzymatic restriction as internal size standards. The contour lengths of the mtDNAs were calibrated against that of ϕX174 Am3 RF DNA in which 10% of the molecules contained a 7% deletion (8).

Gel Electrophoretic Analyses of DNA Fragments. Fragments smaller than about 250 nucleotide pairs would have been un-

* Abbreviations: mtDNA, mitochondrial DNA; *Eco*RI, *E. coli* restriction endonuclease RI; *Hin*dIII, *Haemophilus influenzae*, strain d, restriction endonuclease III; RF DNA, replicative form DNA.

TABLE 1. *Contour length analysis of mtDNAs and the restriction endonuclease fragments*

Source of mtDNA	Contour length compared to φX174 RF DNA[a]	*Eco*RI endonuclease fragment lengths (% genome)[b]	*Hin*dIII endonuclease fragment lengths (% genome)[b]
HeLa	3.08 ± 0.06[c] (61)[d]	6.8 ± 0.4 (272)[d] RI-3[e]	4.9 ± 0.6 (242)[d] H-3[e]
		44.5 ± 0.9 (209) RI-2	32.9 ± 1.3 (108) H-2
		48.6 ± 0.8 (204) RI-1	62.2 ± 2.2 (90) H-1
BSC-1	3.06 ± 0.09 (38)	47.5 ± 1.1 (209) RI-2	5.0 ± 0.8 (88) H-3
		52.5 ± 1.0 (213) RI-1	33.2 ± 1.0 (53) H-2
		—	61.9 ± 1.4 (29) H-1
LA9	3.03 ± 0.07 (61)	12.2 ± 0.6 (155) RI-2	5.0 ± 0.5 (196) H-3
		87.8 ± 2.0 (100) RI-1	11.5 ± 0.7 (145) H-2
		—	83.5 ± 2.9 (68) H-1

[a] These data have been reduced by −0.7% to correct for the presence of a 7% deletion in 10% of the φX174 RF DNA.
[b] 1% of the genome corresponds to 168 base pairs, a value based on a value of 5500 base pairs in the φX174 RF DNA.
[c] Values are expressed as mean ± 1 SD.
[d] Numbers in parentheses indicate the number of mtDNA molecules or fragments measured.
[e] Fragment designation.

detected in the electron microscope analyses. The digests were, therefore, examined in 5% polyacrylamide gels layered over a 10% gel. The fragments were end-labeled with [α-^{32}P]nucleotides incorporated with *E. coli* DNA polymerase I. The procedures for slab gel electrophoresis and autoradiography were those described by Lee and Sinsheimer (11). The method of end-labeling (P. H. Johnson and L. Grossman, manuscript in preparation) consisted of incubating the restriction fragments with *E. coli* DNA polymerase I and a mixture of the four [α-^{32}P]deoxynucleoside triphosphates at 10°. Unincorporated triphosphates were separated from the DNA fragments on a Sephadex G-50 column. Similar analyses were performed on sequential double digests of HeLa and BSC-1 mtDNAs to assess the distance separating restriction sites that were identically situated within the accuracy of the electron microscope method.

RESULTS AND DISCUSSION

Sizing of mtDNAs Compared to φX174 Am3 RF DNA. Nicked mtDNA was mixed with φX174 Am3 RF DNA. At least three φX174 DNA molecules were measured for each mtDNA, as suggested by equation 3 of Davis *et al.* (7). Photomicrographs were taken at the centers of consecutive grid holes. The mtDNA measurements were normalized by φX174 DNA lengths from the same micrograph. The data in Table 1 show that the three mtDNAs have the same mean contour length within ±1% in sets of measurements with individual standard deviations that vary from 2 to 3%.

Sizing of Restriction Endonuclease Fragments. The fragment lengths, normalized to percent genome length, are presented as histograms in Fig. 1. Statistical analyses of these measurements are summarized in Table 1. All three mtDNAs yield three *Hin*dIII fragments that share in common a small (5%) fragment. It is shown later that these fragments are located at the same position in the three genomes. The larger *Hin*dIII fragments of HeLa and BSC-1 mtDNAs are similar in size and in position. HeLa mtDNA yields three *Eco*RI fragments, while BSC-1 and LA9 yield two.

Gel electrophoresis patterns of the six digests showed that small fragments not detectable in the electron microscope and larger than 50 nucleotide pairs were absent. The sensitivity for detection of small fragments was equal to that for the large fragments because of the approximately equal end-labeling with radioactive nucleotides. Small fragments of about 50 nucleotide pairs produced by sequential double digests (see below) were found in the same slab gels in which the analyses of the single digests for small fragments were performed.

Glyoxal Fixation of the D-Loop. The well-documented loss of replicating forms by branch migration processes (9) was prevented by fixation with glyoxal, which reacts with guanylic acid residues in single-stranded DNA (10). The D-loop frequency of glyoxal-fixed woolly monkey mtDNA before and after *Eco*RI digestion remained at 70%, the same value that was observed for unfixed and unrestricted DNA. After digestion of unfixed mtDNA, only 0.1–0.01% of the fragments contained a D-loop, indicating that branch migration occurred almost quantitatively after restriction. It is not known, however, whether the branch migration occurred immediately after restriction or during specimen grid preparation.

Orientation and Direction of Expansion of the D-Loop. When mtDNAs were digested with a restriction endonuclease under conditions known to produce >99% cleavage of all sites, the D-loop was found exclusively on one fragment. This result was apparent upon inspection of the micrographs for all

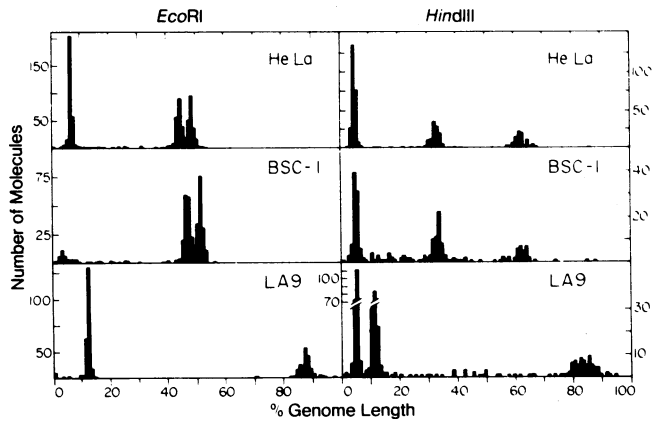

FIG. 1. Histograms of fragments of three mtDNAs obtained with two restriction endonucleases. The lengths are grouped in intervals of 1% of the genome size.

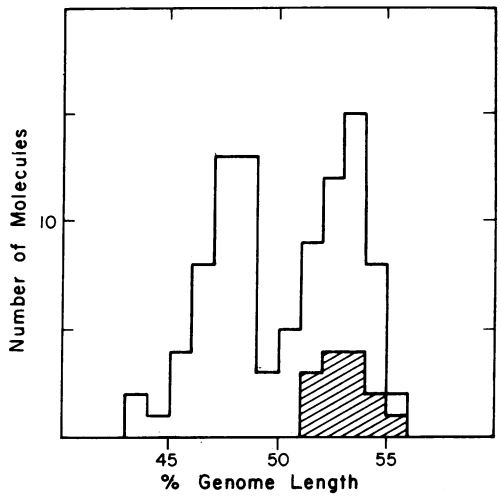

FIG. 2. Length distributions of the fragments produced by *Eco*RI digestion of glyoxal-treated BSC-1 mtDNA. Fragments containing D-loops are indicated by the cross-hatched areas.

mtDNA–enzyme combinations, except for *Eco*RI-digested HeLa and BSC-1. The measured lengths of the two fragments formed in the *Eco*RI–BSC-1 digest form a bimodal histogram (Fig. 2), in which the D-loops are seen to be present only in the larger fragment.

The foregoing type of analysis was impractical with the *Eco*RI–HeLa digest because of the low frequency of D-loop mtDNA. An alternative procedure based on measurements of H-form molecules (Fig. 3) formed by cuts within the D-loop expansions provided an unambiguous specification of the fragment carrying the site for the origin of replication. The length ratios, (A + B)/(D + E) (Fig. 3), calculated from Table 1, are 1.09 ± 0.03 and 0.92 ± 0.02 for the D-loop on the 48.7% (A + B) and 44.5% (D + E) fragment, respectively. In 22 out of a sample of 25 H-form molecules, with the position of the growing point, G, varying from 11 to 94% along the length of (D + E), the ratio was 1.09 ± 0.03. The remaining three had values expected for H-forms containing, in addition, fragment F. We conclude, therefore, that the D-loop is on the largest HeLa fragment, HeLa RI-1.

The length measurements on D-loop-bearing fragments in the six systems (Table 2) show that the position of the D-loop relative to the ends (Fig. 4A), was invariant in each. In order

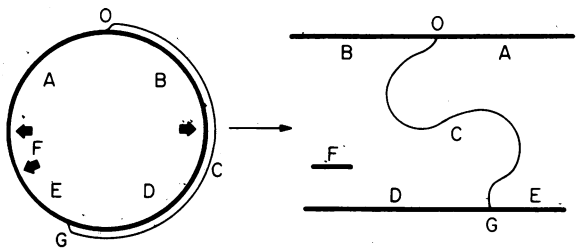

FIG. 3. Diagrammatic representation of the production of H-form molecules derived from replicating intermediates of HeLa mtDNA by *Eco*RI endonuclease action. O and G represent the origin and the growing replication fork, respectively. The small arrows indicate the *Eco*RI sites. For the purpose of the analysis (see text), the placement of fragment F is inconsequential.

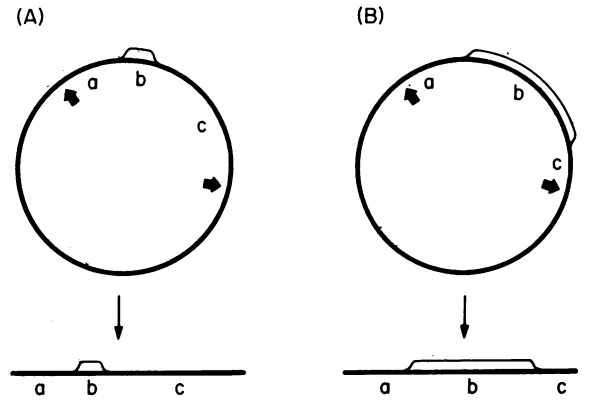

FIG. 4. Diagrammatic representation of the production of fragments containing a D-loop and an expanding D-loop.

to determine the direction of expansion, measurements of lengths *a*, *b*, and *c* (Fig. 4B) were made on expanding D-loop-bearing fragments found in digests of mtDNA originally isolated from the region between the upper and lower bands of buoyant propidium diiodide–CsCl gradients. The length, *a*, was recognized as the constant length in all of the fragments, and this result confirms that expansion is unidirectional. A plot of the data, $(a + b)/\Sigma$ against b/Σ, where Σ is the length of the fragment, is presented in Fig. 5. The linearity confirms that all of the expansions in the *Eco*RI–LA9 digest have begun at a unique position and have expanded unidirectionally (4, 5). Similar results were obtained for the other enzyme–DNA combinations. The ordinate intercepts (Table 2; from Fig. 5 and from data not shown) represent the constant lengths, *a*, adjoining the D-loop. The junction between *a* and the D-loop corresponds to the origin of replication. The satis-

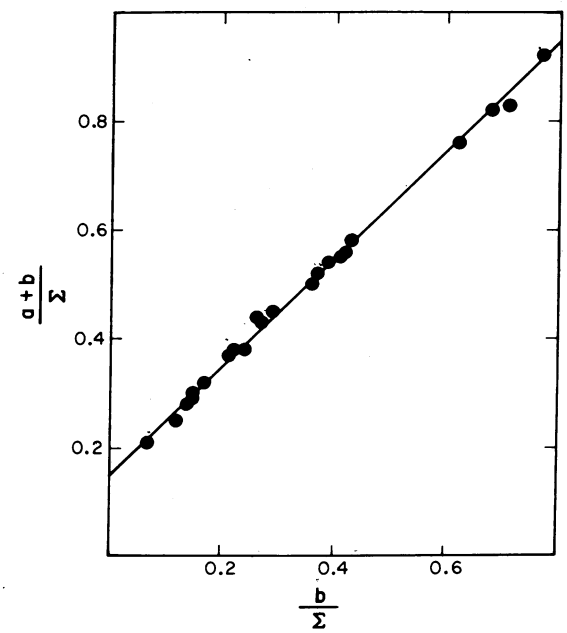

FIG. 5. Measured lengths on limit digested *Eco*RI LA9 mtDNA. The lengths *a* and *b* are defined in Fig. 4B. The indicated lengths are normalized by the length, Σ, of the fragment. The line is the best least squares line and has a slope of unity. The left-most data point, from nonexpanding D-loop molecules (Table 2), was not included in the calculated line.

TABLE 2. *Length analysis of D-loop-containing restriction endonuclease fragments*

mtDNA	Enzyme	Length (expressed as % of total fragment length ± 1 SD)				Ordinate intercept[b]
		a[a]	*b*[a]	*c*[a]		
HeLa	*Eco*RI	49.7 ± 2.0	7.2 ± 1.4	43.1 ± 1.6	(56)[c]	50.4
HeLa	*Hin*dIII	60.0 ± 2.6	5.7 ± 1.4	34.3 ± 2.0	(12)	61.6
BSC-1	*Eco*RI	52.9 ± 1.3	7.5 ± 1.3	39.6 ± 1.1	(16)	50.9
BSC-1	*Hin*dIII	58.8 ± 1.3	6.4 ± 0.8	34.8 ± 1.0	(44)	61.9
LA9	*Eco*RI	14.6 ± 0.7	3.8 ± 0.6	81.6 ± 0.9	(58)	15.2
LA9	*Hin*dIII	70.4 ± 0.8	4.4 ± 0.7	25.2 ± 1.1	(15)	71.4

[a] The lengths *a*, *b*, and *c* correspond to those designated as such in Fig. 4A.
[b] From Fig. 5 and data (not shown).
[c] Numbers in parentheses indicate the number of mtDNA fragments measured.

factory agreement between the values of *a* and the ordinate intercepts (Table 2) is noted.

Determination of the Fragment Order. Fragment orders for the mtDNAs containing three restriction sites have been derived from incompletely digested mtDNAs, as illustrated diagrammatically in Fig. 6. The two possible orders, BCA and ACB, where A < B < C, were distinguished by measurements on D-loop-bearing molecules. Of the three permuted full-length molecules, only type a molecules were useful in the analyses. The short lengths measured from the fixed fork of the D-loop to the terminus of *Hin*dIII-digested mtDNAs from HeLa, BSC-1, and LA9 cells were 22.2 ± 0.9, 23.3 ± 0.8, and 23.7 ± 0.6 cm, respectively. The calculated values from the data (Tables 1 and 2) were 22.8 ± 2.1, 23.4 ± 1.6, and 23.8 ± 1.5 cm, respectively, for the order BCA and 32.2 ± 1.7, 31.8 ± 1.5, and 28.9 ± 1.7 cm, respectively, for the order ACB. We conclude that the order BCA is correct in all three cases. This conclusion was corroborated by measurements on the longer dimension of these molecules, and also by measurements of the molecules with one fragment missing, (d and e, Fig. 6).

In *Eco*RI-digested HeLa mtDNA, the fixed end of the D loop occurs at the midpoint of the largest fragment, a result that renders inapplicable the analyses used above. However, the D loop will expand into the longer segment if the order is ACB. Two expansions indicating this order were found. Eleven expansions in molecules of types d and e (Fig. 6) showed unequivocally that the order is indeed ACB. No molecules were found that indicated the alternative order.

Since both BSC-1 and LA9 mtDNAs yielded only two fragments when digested with the *Eco*RI enzyme, the complete maps were determined with the data presented in the previous section in which the location and direction of expansion of the D-loop on one fragment were evaluated.

Cleavage Maps of the Three mtDNAs. All three mtDNAs (Fig. 7) contain the hexanucleotide sequences recognized by *Hin*dIII at two corresponding positions on the genome (25% and 30%), a result that suggests that these sequences occur in an evolutionarily conserved section of the genome. In addition, the third *Hin*dIII site on HeLa and BSC-1 is also in common at 63%. One *Eco*RI recognition site, at 24%, occurs in both HeLa and BSC-1 mtDNAs. No other *Eco*RI sites are in common.

The results for all combinations of enzymes and mtDNAs are shown in Fig. 7. As a check on the correctness of the independently derived *Eco*RI and *Hin*dIII maps of LA9 mtDNA, a *Hin*dIII digest was exhaustively digested with *Eco*RI endonuclease. The resulting D-loop-bearing fragment length was 37 ± 1%, as compared with 38% (Fig. 7), and 74% if the direction of expansion had been incorrectly assigned.

The accuracy of the position of the restriction sites presented in Fig. 7 is estimated to be ±1% of the genome. An

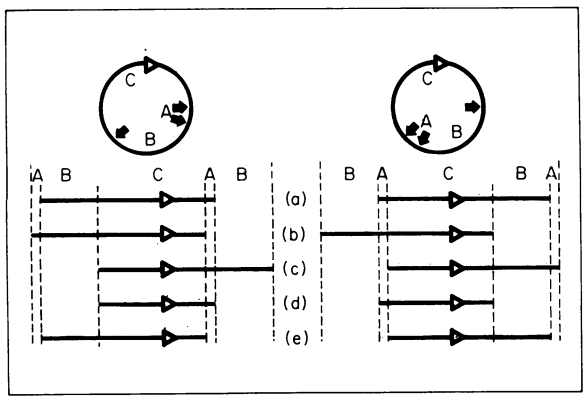

FIG. 6. Diagrammatic representation of the formation of permuted fragments of HeLa, BSC-1, and LA9 mtDNAs upon incomplete digestion with *Hin*dIII endonuclease. The triangle indicates the D-loop and points in the direction of expansion. The dashed lines indicate the restriction sites for the alternative orders BCA and ACB.

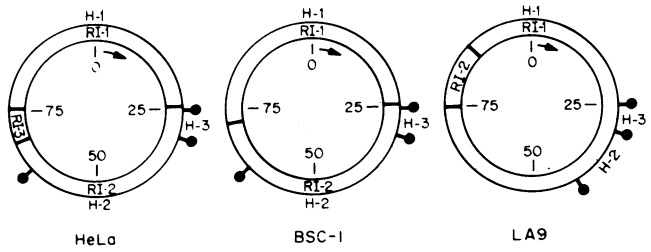

FIG. 7. Cleavage maps of three mtDNAs. O represents the origin of replication, the fixed fork of the D-loop, and the arrow represents the direction of replication. The *Eco*RI restriction sites are shown within the concentric circles. The *Hin*dIII sites are indicated by the symbol ↑. The positions of the sites for both enzymes at 25 map units in BSC-1 and HeLa mtDNAs are closer to each other than indicated, and are within 50 nucleotide pairs, as demonstrated by gel electrophoretic analyses of sequential digests by both enzymes (see text).

*Eco*RI and a *Hin*dIII site occur at 24.5 and 25.0 map units in the cleavage of HeLa and BSC-1, respectively. The assignment of the positions of these restriction sites was checked by polyacrylamide electrophoresis of double digests of each of these DNAs. A single small fragment containing $\leqslant 50$ nucleotide pairs was found in each of the double digests. The same results were obtained upon changing the order of the sequential endonuclease digestions.

The maps presented in Fig. 7 can serve as primary references for further, more detailed mapping with other restriction enzymes, and for positioning mitochondrial RNAs relative to the origin of replication. The maps are currently in use in the analyses of the structure of *in vitro* plasmid–mtDNA recombinants grown in and isolated from *E. coli* (W. Brown, K. Tait, H. Boyer, and J. Vinograd, unpublished).

We thank H. W. Boyer, University of California, San Francisco, and P. H. Johnson for generously providing enzymes, Denzille Stephens for assistance in cell culture, and Frank Mayer for assistance in measuring molecules. We also thank D. Clayton and D. Robberson for informing us of their preliminary results on the *Eco*RI maps of mouse and human mtDNAs. This work was supported in part by USPHS NIH Grants GM15327 and CA08014 and by a National Science Foundation Training Grant to W.M.B. This is contribution no. 4962 from the Division of Chemistry and Chemical Engineering.

1. Smith, H. O. & Nathans, D. (1973) "A suggested nomenclature for bacterial host modification and restriction systems and their enzymes," *J. Mol. Biol.* **81**, 419–423.
2. Kasamatsu, H., Robberson, D. L. & Vinograd, J. (1971) "A novel closed-circular mitochondrial DNA with properties of a replicating intermediate," *Proc. Nat. Acad. Sci. USA* **68**, 2252–2257.
3. Robberson, D. L., Kasamatsu, H. & Vinograd, J. (1972) "Replication of mitochondrial DNA. Circular replicative intermediates in mouse L cells," *Proc. Nat. Acad. Sci. USA* **69**, 737–741.
4. Kasamatsu, H. & Vinograd, J. (1973) "Unidirectionality of replication in mouse mitochondria DNA," *Nature New Biol.* **241**, 103–105.
5. Robberson, D. L. & Clayton, D. A. (1972) "The replication of mitochondrial DNA in mouse L cells and their thymidine kinase minus derivatives: Displacement replication on a covalently-closed circular template," *Proc. Nat. Acad. Sci. USA* **69**, 3810–3814.
6. Smith, C. A., Jordan, J. M. & Vinograd, J. (1971) "*In vivo* effects of intercalating drugs on the superhelix density of mitochondrial DNA isolated from human and mouse cells in culture," *J. Mol. Biol.* **59**, 255–272.
7. Davis, R. W., Simon, M. & Davidson, N. (1971) in *Methods in Enzymology*, eds. Grossman, L. & Moldave, K. (Academic Press, New York), Vol. 21, pp. 413–428.
8. Zuccarelli, A. J., Benbow, R. M. & Sinsheimer, R. L. (1972) "Deletion mutants of bacteriophage ϕX174," *Proc. Nat. Acad. Sci. USA* **69**, 1905–1910.
9. Robberson, D. L. & Clayton, D. A. (1973) "A genetically distinct thymidine kinase in mammalian mitochondria," *J. Biol. Chem.* **248**, 4512–4514.
10. Broude, N. E. & Budowsky, E. I. (1971) "The reaction of glyoxal with nucleic acid components III. Kinetics of the reaction with monomers," *Biochim. Biophys. Acta* **254**, 380–388.
11. Lee, A. S. & Sinsheimer, R. L. (1974) "A cleavage map of bacteriophage ϕX174 genome," *Proc. Nat. Acad. Sci. USA* **71**, 2882–2886.